E-Journal of Advanced Maintenance Vol.7-1 (2015) 129-137
Japan Society of Maintenology

Statistical Model of Micro Crack Growth for the Evaluation of Accumulated Fatigue in NPPs

Shigeki ABE[1,*], Takao NAKAMURA[1] and Masayuki KAMAYA[2]

[1] *Osaka University, 2-1 Yamadaoka Suita, Osaka, Japan*
[2] *Institute of Nuclear Safety System, Inc, 64 Sata, Mihama-cho, Mikata-gun, Fukui 919-1205, Japan*

ABSTRACT

In order to establish sophisticated management of aging degradation and to achieve high reliability of components in nuclear power plants, it is required to reveal the mechanism of aging degradation and to quantify its deterioration. In low-cycle fatigue regime, it was shown that the number of cycles to specimen failure (fatigue life) can be estimated by predicting crack growth. The application of crack length for representing fatigue damage will make it possible to measure fatigue damage by inspection. In previous study, crack growth with inhomogeneous rate and fatigue life in a typical condition were predicted with statistical model of micro crack growth. In this study, fatigue test in expanded condition was conducted in air at room temperature in order to define the relationship between damage factor (*DF* = number of cycles/fatigue life) and crack length. Crack initiation and crack propagation during fatigue test were measured by replica investigation periodically. Statistical model of micro crack growth was applied to the observation result and its applicability for various strain ranges was demonstrated. The relationship between the damage factor and crack length was shown and its use for maintenance was discussed.

KEYWORDS

Nuclear power plants, fatigue damage, low-cycle fatigue, crack initiation, crack growth

ARTICLE INFORMATION

Article history:
Received 17 November 2014
Accepted 28 April 2015

1. Introduction

In order to establish sophisticated management of aging degradation and to achieve high reliability of components in nuclear power plants (NPPs), it is required to reveal the mechanism of aging degradation and to quantify the magnitude of the degradation. In low-cycle fatigue regime, it was shown that the number of cycles to specimen failure (fatigue life) can be estimated by predicting crack growth. It means that fatigue damage can be represented by crack length [1]. Therefore, the fatigue damage can be estimated by measuring the crack size. Namely, the fatigue damage of NPP components can be measured by inspections [2]. However, the crack growth behavior has statistical nature and is difficult to predict by deterministic evaluation. In this study, the statistical crack growth was predicted by a Monte Carlo simulation. First, crack initiation and propagation behaviors were observed during a low-cycle fatigue tests. Then, the initiation and propagation was quantified and applied to the Monte Carlo model for crack growth from microscopic size. The relationship between the damage factor (*DF* = number of cycles/fatigue life) and crack length was then set up. It was discussed that the relationship can be applied for the evaluation of fatigue damage accumulated in NPP components.

2. Crack Growth during Fatigue Tests

2.1. Crack Growth Investigation during Fatigue Tests

Crack growth during fatigue test ($\Delta\varepsilon = 1.2\%$) has been observed in previous study [3]. In this study, crack growth during fatigue test of $\Delta\varepsilon = 0.8\%$ was observed. Test results obtained in the

* Corresponding author, E-main: s-abe@ne.see.eng.osaka-u.ac.jp

previous study [3] was also subjected to statistical analysis.

The material used for the fatigue tests was solution heat-treated Type 316 austenitic stainless steel. The geometry of test specimen was shown in Fig.1. Chemical composition and mechanical properties were shown in Tables 1 and 2. Pull-push axial strain-controlled fatigue test was conducted in room temperature laboratory environment using servo-electric test machine. Strain range was controlled to 0.8% under a constant strain rate of 0.4%/s. The crack growth during the tests was monitored by taking replicas of specimen surface using acetyl cellulose films in every 500 cycles. The observed area was 3×6 mm^2 on the surface of test specimens. Cracks of less than 20 μm could be identified. Total 166 cracks were observed in the observed area. Fig.2 shows the change of crack length of main crack, which caused specimen failure, together with that of five cracks arbitrary chosen. Fig.3 also shows the crack growth in previous study obtained for $\Delta\varepsilon$ =1.2%. The crack initiations are not the same and the propagation rate varied significantly even for the main crack.

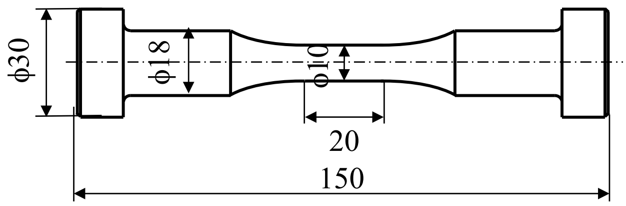

Fig. 1 Geometry of test specimen (unit: mm).

Table 1 Chemical content of test material (wt%)

Fe	C	Si	Mn	P	S	Ni	Cr	Mo
Bal.	0.06	0.5	1.3	0.031	0.027	10.18	16.94	2.02

Table 2 Mechanical properties of test material (R.T.)

0.2% proof strength	Tensile strength	Young's modulus	Elongation
297MPa	611MPa	202.5GPa	0.58

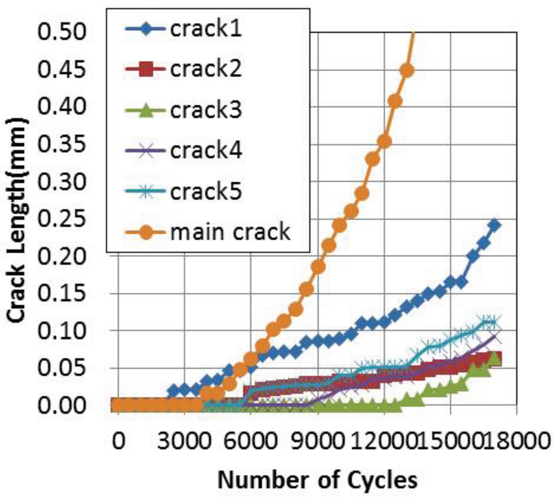

Fig.2 Inhomogeneous crack growth in observation area ($\Delta\varepsilon$ = 0.8%).

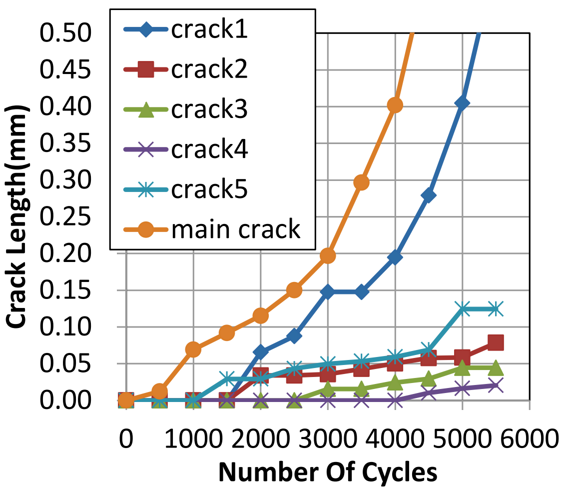

Fig.3 Inhomogeneous crack growth in observation area ($\Delta\varepsilon$ = 1.2%).

2.2. Quantification of Initiation and Growth Behavior

2.2.1. Crack initiation

The change in the number of cracks obtained for $\Delta\varepsilon$=0.8% and 1.2% are shown in Figs.4 and 5, respectively. The cracks were initiated with various incubation period. Cracks were found in the first replica and were initiated continuously until the end of the tests. Number of cracks was about 230 at 5,000 cycles under $\Delta\varepsilon$ = 1.2%, whereas it was less than 20 under $\Delta\varepsilon$ = 0.8%.

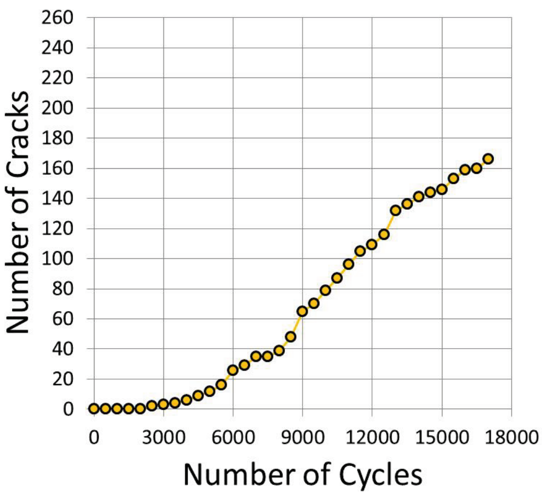

Fig.4 Change in number of cracks in the observation area ($\Delta\varepsilon$ =0.8%).

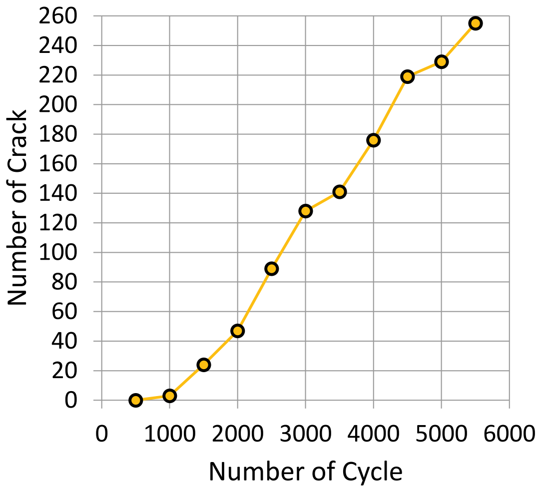

Fig.5 Change in number of cracks in the observation area ($\Delta\varepsilon$ =1.2%).

2.2.2. Crack propagation

Crack propagation rates in the depth direction were calculated assuming that the ratio of crack depth to crack surface length equals to 0.5. Observation of fractured surface revealed that the aspect ratio was almost 0.5 [4]. Fig.6 shows the relationship between the crack propagation rates in the depth direction obtained for $\Delta\varepsilon = 0.8\%$ and range of equivalent stress intensity factor, which is defined by [2]:

$$\Delta K_{eq} = f \Delta\varepsilon E \sqrt{\pi a} \quad (1)$$

$$f = 0.8379\left(\frac{a}{R}\right)^3 - 0.6486\left(\frac{a}{R}\right)^2 + 0.4128\left(\frac{a}{R}\right) + 0.6103 \quad (2)$$

where E and a are Young's modulus and crack depth, respectively. Equation (2) for calculating f corresponded to the configuration of the specimen with surface crack [2]. R is radius of the specimen. It has been shown that the equivalent stress intensity factor had good correlation with crack propagation rates even in the low-cycle regime [4,5]. From the regression of the obtained results, crack propagation rate da/dN for this material has been obtained [2]:

$$\frac{da}{dN} = 3.33 \times 10^{-12} \left(\Delta K_{eq}\right)^{2.85} \quad (3)$$

where growth rate da/dN given in m/cycle and ΔK_{eq} in MPa m$^{0.5}$. The relationship between crack propagation rates in depth direction and surface crack lengths is shown in Fig.8. Crack propagation rates tended to be faster than crack propagation rates given by equation (3) and showed eminent scatter when the crack size was relatively small. For the comparison, the growth rates for $\Delta\varepsilon = 1.2\%$ also shows in Figs. 7 and Fig. 9.

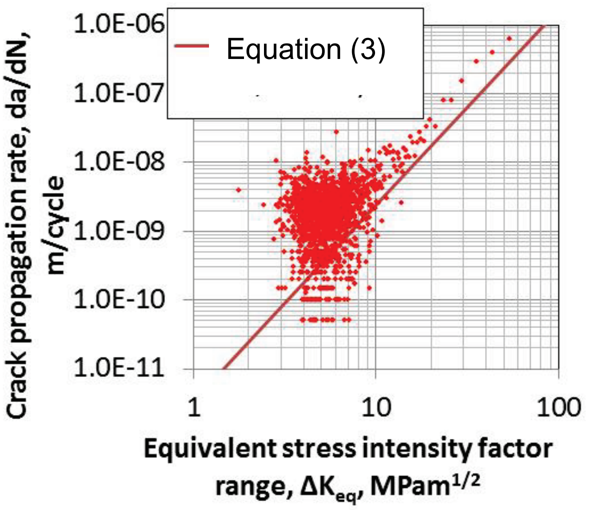

Fig.6 Relationship between crack propagation rate and equivalent stress intensity factor ($\Delta\varepsilon$ =0.8%).

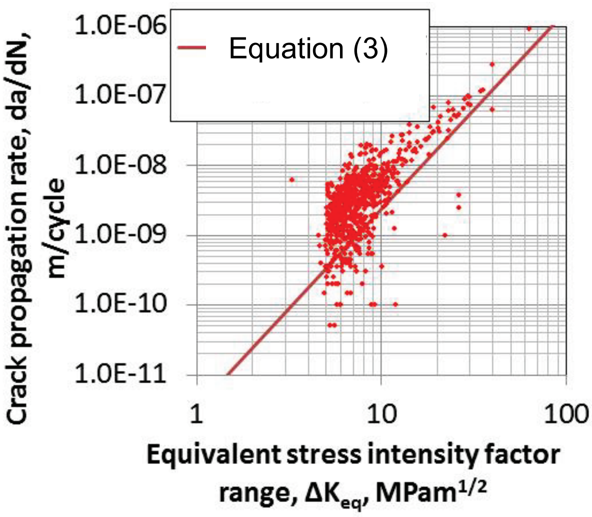

Fig.7 Relationship between crack propagation rate and equivalent stress intensity factor ($\Delta\varepsilon$ =1.2%).

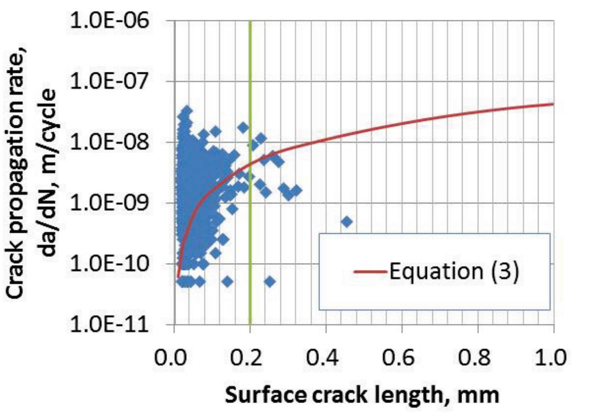

Fig. 8 Relationship between crack propagation rate and surface crack length ($\Delta\varepsilon$ =0.8%).

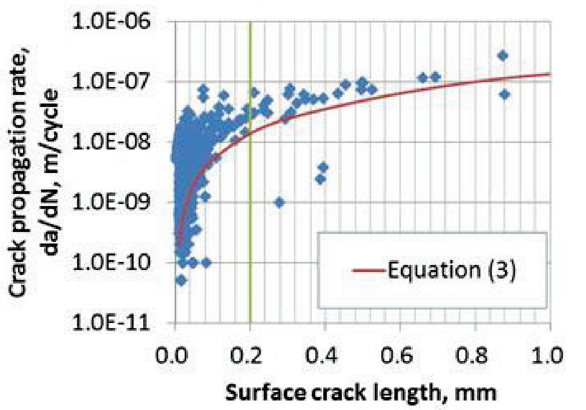

Fig. 9 Relationship between crack propagation rate and surface crack length ($\Delta\varepsilon$ =1.2%).

3. Statistical Model of Micro crack growth

3.1. Quantification

3.1.1. Crack initiation

Crack initiation was defined as the number of cycles when crack length of more than 20 μm was observed. The cracks more than 20 μm could be identified as a crack. The relationship between incubation period and the number of cracks normalized by the value at the fatigue life is shown in Fig.10. The regression of the relationship was obtained by equation (4). For the comparison, the relationship and regression for $\Delta\varepsilon$ = 1.2% are shown in Fig. 11 and equation (5), respectively.

$$N_i = 14913 \times n_{total.norm}{}^{0.3579} \qquad (4)$$

$$N_i = 5375.3 \times n_{total.norm}{}^{0.4123} \qquad (5)$$

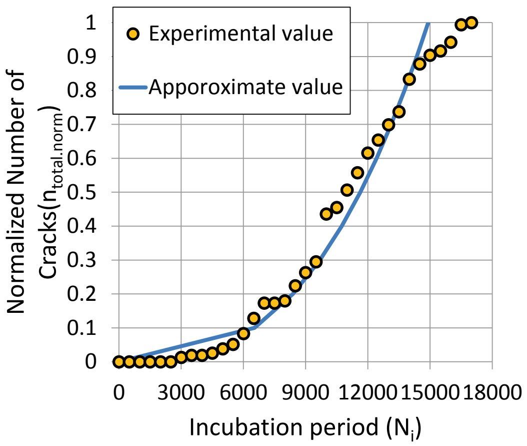

Fig.10 Relationship between incubation period and number of cracks ($\Delta\varepsilon$ =0.8%).

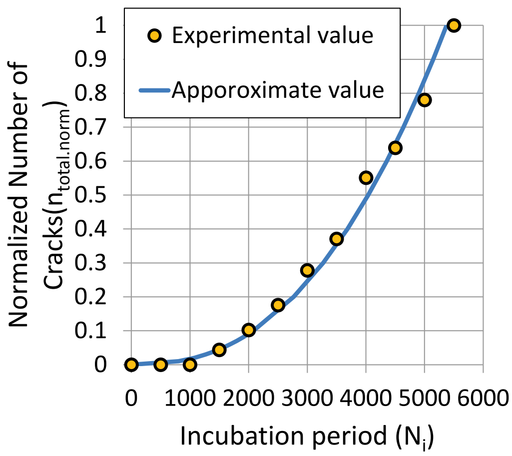

Fig.11 Relationship between incubation period and number of cracks ($\Delta\varepsilon$ =1.2%).

3.1.2. Crack propagation

In order to reflect the relatively fast crack propagation rates and scattered propagation rate of the micro cracks, 180 μm was taken as threshold length for stable crack propagation. Then, variation in the crack propagation rates for cracks under the threshold length was investigated. The crack propagation rates were calculated every 40 μm from the crack initiation. Namely, the averaged propagation rates during the crack growing from 20-60 μm, 60-100 μm, 100-140 μm and 140-180 μm were calculated. The length of 40 μm represents average grain size of test material. Figure 12 depicted how the crack propagation rate was calculated. Since averaged crack growth rates in each section were almost linear in log-normal plot, it was assumed that the distribution of crack propagation rates followed log-normal distribution, and average crack propagation rate and standard deviation were obtained as shown in Tables 3 and 4. Equation (6) was obtained by the least-square fit of the relationship between equivalent stress intensity factor and averaged crack propagation rate. Variation of crack propagation rate was considered by giving log-normal distribution for equation (6). Figs. 13 and 14 show the variation range of the crack propagation rates and averaged crack propagation rates. The dispersion reflects the relatively fast crack propagation rate and their large dispersion in micro crack growth region.

$$\frac{da}{dN} = 2.05\times10^{-11}\left(\Delta K_{eq}\right)^{2.50} \qquad (6)$$

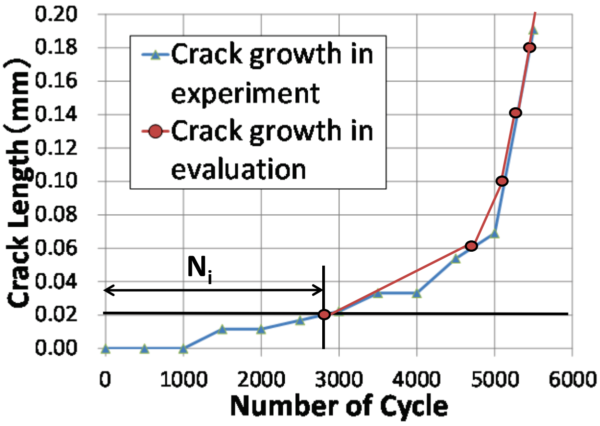

Fig. 12 Simplification in the process of crack growth for the evaluation.

Table 3 Dispersion of crack propagation rate ($\Delta\varepsilon$ = 0.8%, σ: standard deviation)

Table 4 Dispersion of crack propagation rate ($\Delta\varepsilon$ = 1.2%, σ: standard deviation)

Crack Length (mm)	0.02～0.06	0.06～0.10	0.10～0.14	0.14～0.18
da/dN (average)	2.33E-08	6.01E-08	5.99E-08	9.86E-08
σ	0.320	0.599	0.255	0.189

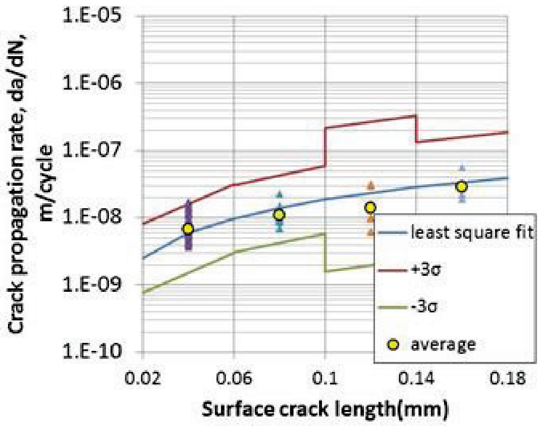

Fig.13 Dispersion of crack propagation rate ($\Delta\varepsilon$ =0.8%).

Crack Length (mm)	0.02～0.06	0.06～0.10	0.10～0.14	0.14～0.18
da/dN (average)	6.75E-09	1.11E-08	1.40E-08	2.87E-08
σ	0.170	0.166	0.357	0.226

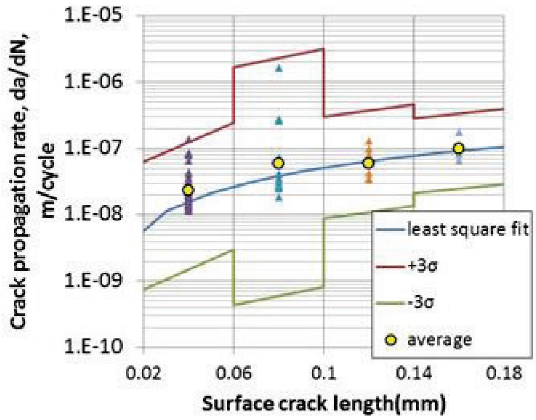

Fig.14 Dispersion of crack propagation rate ($\Delta\varepsilon$ =1.2%).

3.2. Monte Carlo Model for Micro Crack Growth

Based on quantified crack initiation and crack propagation, a Monte Carlo model to simulate the micro crack initiation and growth behaviors was developed. The flow of simulation is shown in Fig. 15. First, number of cracks was determined, and incubation period and crack propagation rate in each section were given by using equations (4) and (5) using the constant given by Tables 3 and 4. The dispersion in the growth rate was not considered for the cracks more than 180 μm in depth, because the dispersion was judged to be negligibly small.

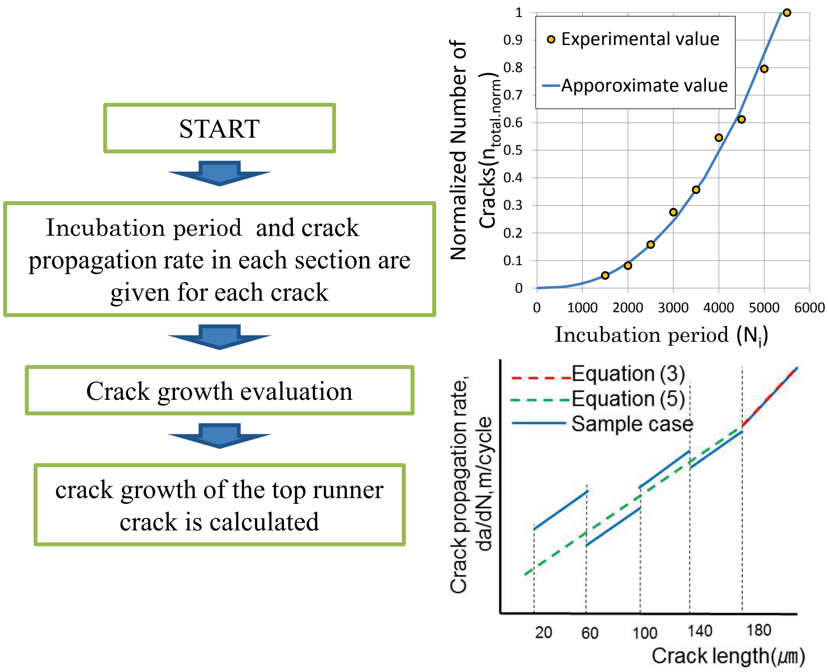

Fig.15 Statistical model of micro crack growth.

4. Fatigue Crack Growth Prediction by Crack Growth model

From observation result, number of cracks initiated in the whole specimen was deduced to be about 6,000. Then, the simulation was conducted for 6,000 cracks for single specimen. Fatigue life

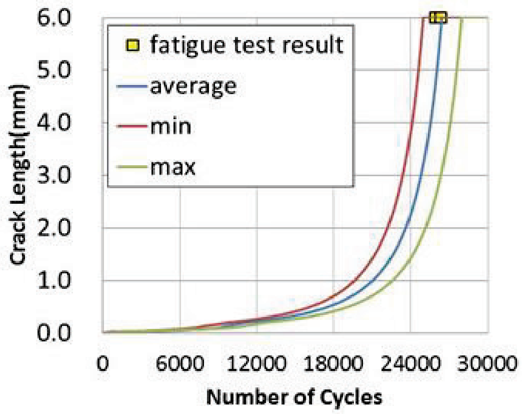

Fig.16 Dispersion of crack growth ($\Delta\varepsilon$ =0.8%). (min: minimum fatigue life, max: maximum fatigue life)

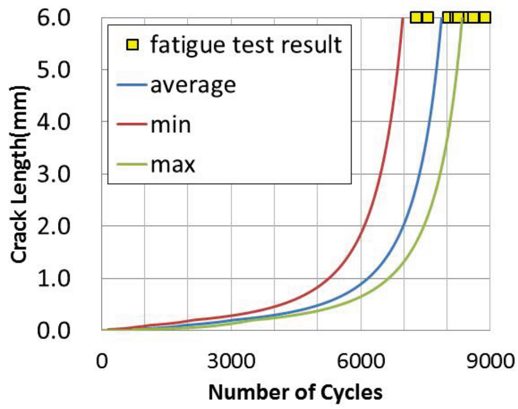

Fig.17 Dispersion of crack growth ($\Delta\varepsilon$ =1.2%). (min: minimum fatigue life, max: maximum fatigue life)

was defined as the number of cycles when a crack reached to 3 mm in depth first. The fatigue lives were calculated for 100 specimens. Growth of the maximum crack for each specimen is shown in Figs. 16 and 17, in which the fastest, slowest and the averaged crack growth in 100 specimens are shown. Fatigue lives obtained by low-cycle fatigue tests were also shown in these figure. The number of low-cycle fatigue test results are 2 and 10 for $\Delta\varepsilon$ = 0.8% and $\Delta\varepsilon$ = 1.2%, respectively. Predicted fatigue lives and their dispersion were comparable with the test results.

5. Discussion

5.1. Relationship between *DF* and crack length

The Monte Carlo model for micro crack growth was developed in order to simulate surface crack initiation and growth in test specimen. Predicted fatigue lives and their dispersion in this model agreed well with the result of fatigue tests. The relationship between the damage factor and crack lengths were shown in Figs.18 and 19, which are obtained using the results shown in Figs.16 and 17. There is a little difference in the relationship between *DF* and crack length. It is because the fatigue life can be estimated by predicting crack propagation. In high cycle fatigue regime, it is deduced that the incubation period becomes longer than that obtained in the current tests. In order to develop a comprehensive model applicable to various strain ranges, statistical crack initiation behavior should be quantified and modeled for smaller strain range.

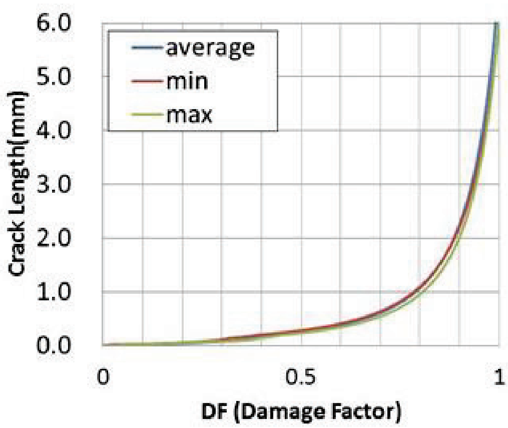

Fig.18 Dispersion of P-curve ($\Delta\varepsilon$ =0.8%).

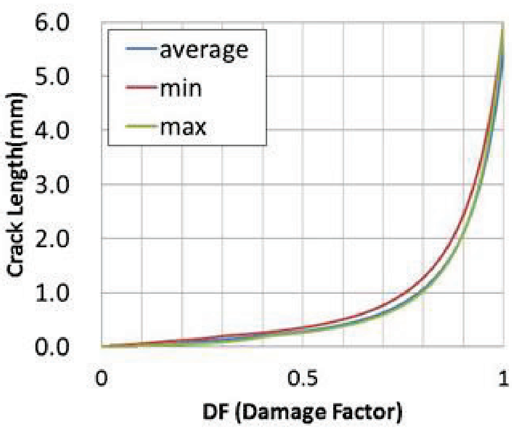

Fig.19 Dispersion of P-curve ($\Delta\varepsilon$ =1.2%).

5.2. Application to in-service inspection

Using the relationship between *DF* and crack length, which is referred to as P-curve, the accumulated fatigue damage can be estimated from the detected size of a crack or, if no crack is detected, the damage is estimated from the detectable crack size of applied inspection technique. Flaw detectability of inspection technique is represented by *POD* (Probability of Detection) for crack size. The crack size was correlated to *DF* by the P-curve. Then, by combining the *POD* curve and P-curve, the PD curve is obtained as shown in Fig.20. The PD curve informs that, the *DF* was less than 0.7 at the maximum case if no crack was found by the inspection as shown in Fig.20. In other words, the remaining fatigue life was more than 30% of the total fatigue life. Improvement of the inspection technique can extend the expected fatigue life. As most inspection program for power plants do not detect cracks, it is important to make an interpretation for the fact that no cracking was found.

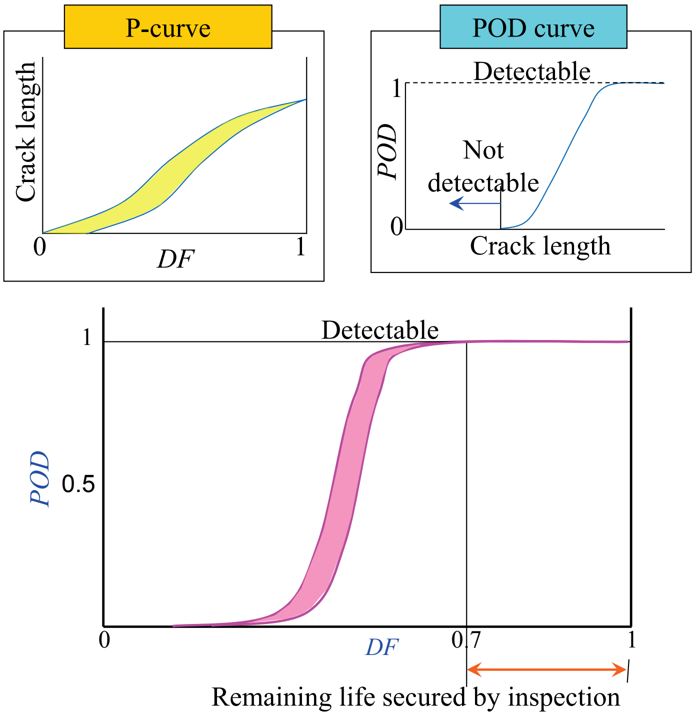

Fig.20 Development of PD curve.

6. Conclusion

In order to quantify the fatigue crack initiation and growth behaviors, fatigue test was conducted in air at room temperature. Based on crack initiation and crack propagation behavior observed in the fatigue test, a Monte Carlo model for simulating crack initiation and growth from microscopic size was developed. The following results could be drawn.

- Initiation and growth of 166 cracks were examined by replica investigations. The continuous crack initiation and scattered propagation rates were observed.
- The average and dispersions of incubation period and crack propagation rates were quantified using the test results.
- Statistical model of micro crack growth was set up based on quantified crack initiation and crack propagation. Inhomogeneous crack growth in fatigue test was simulated by the crack growth in this model.
- Dispersion of fatigue life in 100 cases was predicted. Predicted fatigue lives and their dispersion agreed well with those of fatigue tests.
- The relationship between the damage factor (*DF* = number of cycles/fatigue life) and crack length was clarified and its application for the evaluation of accumulated fatigue in NPPs was discussed.

Acknowledgement

This work has been performed as a part of the Japan Ageing Management Program on System Safety (JAMPSS) sponsored by Nuclear Regulation Authority (NRA).

References

[1] Murakami, Y. and Miller, K.J., 2005, What is fatigue damage? A view point from the observation of low cycle fatigue process, International Journal of Fatigue, 27, pp.991-1005.
[2] M. Kamaya and T. Nakamura, A flaw tolerance concept for plant maintenance using virtual fatigue crack growth curve, Proceedings of ASME PVP2013 – 97851.
[3] S. Abe and T. Nakamura, Statistical model of micro crack growth for the evaluation of accumulated fatigue in NPPs, Proceedings of ASME PVP2014 – 28603.
[4] M. Kamaya and M. Kawakubo, 2012, Strain-based modeling of fatigue crack growth – An experimental approach for stainless steel, International Journal of Fatigue, 44, pp.131-140.
[5] M. Kamaya, M. Kawakubo, "Damage assessment of low-cycle fatigue by crack growth prediction (development of growth prediction model and its application)", Transactions of the Japan Society of Mechanical Engineers Ser. A, Vol. 78 pp. 1518-1533 (2012).